Variability of rainfall rate and raindrop size distributions in heavy rain

James A. Smith,[1] Eric Hui,[1] Matthias Steiner,[2] Mary Lynn Baeck,[1]
Witold F. Krajewski,[3] and Alexandros A. Ntelekos[1]

Received 15 January 2008; revised 25 November 2008; accepted 14 January 2009; published 29 April 2009.

[1] A stochastic model of rainfall rate is used to examine the temporal variability of rainfall during heavy convective rain periods. The model represents the microstructure of rainfall rate at time scales that are important for land surface processes associated with infiltration and runoff production. The representation of rainfall rate is based on a marked point process model of raindrop size distributions, which yields a gamma raindrop spectrum with parameters that are time-varying stochastic processes. Raindrop size distribution observations from a Joss-Waldvogel disdrometer in Princeton, New Jersey, during the period May–October 2006 are used along with the stochastic model to examine rainfall rate variability. Analyses focus on a sample of 60-min time periods in which heavy convective rainfall occurred. Central elements of the analyses entail examination of the relationships between rainfall rate and the time-varying model parameters that characterize the raindrop size distribution. We also examine the dependence structure among these processes. "Scaling law" formulations of raindrop size distributions are used to examine variability of raindrop size distributions. Analyses of the Princeton heavy rainfall periods also point to seasonal and diurnal heterogeneities as important elements of the distribution of extreme rainfall rates. Convective intensity, as reflected in cloud-to-ground lightning observations, plays an important role in the distribution of extreme rainfall rates and the evolution of raindrop size distributions associated with heavy rainfall.

Citation: Smith, J. A., E. Hui, M. Steiner, M. L. Baeck, W. F. Krajewski, and A. A. Ntelekos (2009), Variability of rainfall rate and raindrop size distributions in heavy rain, *Water Resour. Res.*, *45*, W04430, doi:10.1029/2008WR006840.

1. Introduction

[2] A stochastic model of rainfall rate is used to examine the temporal variability of rainfall during heavy convective rain periods. The representation of rainfall rate is based on a marked point process model of raindrop size distributions [*Smith*, 1993; see also *Uijlenhoet et al.*, 2003a, 2003b; *Steiner and Smith*, 2004], which yields a gamma raindrop spectrum $N(x|N_0, \Lambda, \mu)$ (drops m^{-3} mm^{-1}) with parameters that are time-varying stochastic processes:

$$N(x \mid N_0(t),\ \Lambda(t), \mu(t)) \ = \ N_0(t)\ x^{\mu(t)} \exp(-\Lambda(t)x) \qquad (1)$$

The stochastic model of rainfall rate takes the form

$$R(t) = \frac{6\pi\ v_0}{10^4}\ \Gamma(4 + \mu(t) + p)\ N_0(t)\ \Lambda(t)^{-(4+\mu(t)+p)}; t \in [0, T] \qquad (2)$$

where R(t) is rainfall rate (mm h^{-1}) at time t, v_0 and p are "terminal velocity " parameters (see section 2), $\Gamma(s)$ is the gamma function and the time interval is denoted $[0, T]$.

[3] Raindrop size distribution observations from a Joss-Waldvogel disdrometer [*Joss and Waldvogel*, 1967; see also *Steiner et al.*, 2004; *Tokay et al.*, 2005; *Munchak and Tokay*, 2008] for recent treatments of raindrop size distribution measurements) in Princeton, New Jersey, during the period May–October 2006 are used along with the stochastic model to examine rainfall rate variability. Analyses focus on a sample of 60-min time periods in which heavy convective rainfall occurred. The time interval T of 60 min corresponds to periods in which one or more convective elements pass over the disdrometer location. Cloud-to-ground lightning observations from the National Lightning Detection Network (NLDN) [see *Orville and Huffines*, 2001] are used to show that convective intensity (see *Zipser et al.* [2006] for discussion of measures of convective intensity) plays an important role in the distribution of extreme rainfall rates and the evolution of raindrop size distributions for heavy rainfall.

[4] The model represents the microstructure of rainfall rate at time scales that are important for land surface processes associated with infiltration and runoff production. In formulations of infiltration and saturated-unsaturated zone flow based on the Richards equation [*Celia et al.*, 1990; *Williams and Miller*, 1999], rainfall rate provides a surface boundary condition. Nonlinearity of the Richards equation

[1]Department of Civil and Environmental Engineering, Princeton University, Princeton, New Jersey, USA.
[2]Research Applications Laboratory, National Center for Atmospheric Research, Boulder, Colorado, USA.
[3]IIHR-Hydroscience and Engineering, University of Iowa, Iowa City, Iowa, USA.

0043-1397/09/2008WR006840

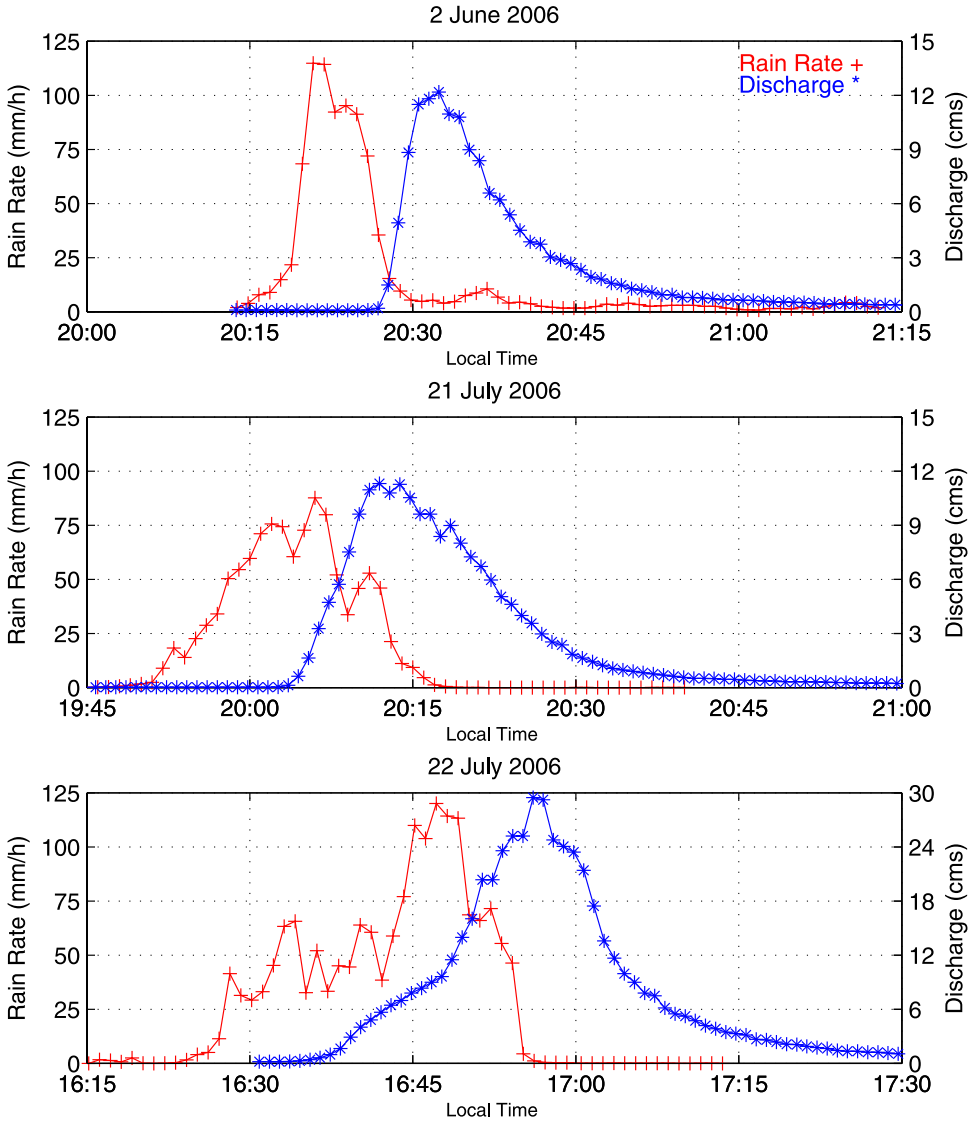

Figure 1. Time series of rainfall rate (mm h^{-1} from disdrometer) and "unit discharge" (discharge in m^3 s^{-1} divided by drainage area (in km^2)) for (top) 2 June, (middle) 21 July, and (bottom) 22 July. Note the different discharge range for the 22 July storm, relative to the 2 June and 21 July storms.

makes the dependence on rainfall microstructure an important element of infiltration and runoff production.

[5] The dependence of runoff processes on rainfall microstructure is especially important for extreme rainfall rates in small urban catchments. In these settings, rainfall microstructure plays a central role in controlling flood hazards. Rainfall rate and discharge time series (Figure 1) for the three events that produced the largest flood peaks in Harry's Brook (see section 3) during the summer 2006 observing period illustrate the close relationship between rainfall rate variability and urban flooding. Harry's Brook drains the urban core of Princeton and has a drainage area of 1.1 km^2. The 22 July 2006 storm produced a unit discharge peak of 26.5 m^3 s^{-1} km^{-2} (at a drainage area of 1.1 km^2) from a 27-min period with 1-min rainfall rates greater than 25 mm h^{-1} and a peak 1-min rainfall rate of 120 mm h^{-1}. The unit discharge peak from the 22 July storm period is comparable to record flood peaks in small urban catchments from locations throughout the United s [*Smith et al.*, 2005]. Storm total rainfall for the 22 July period was 28.7 mm and the storm total runoff was 27.6 mm for a runoff ratio of 97%. Runoff ratios for the 2 June and 21 July storm periods shown in Figure 1 were both 56%. Runoff ratios for other events during the warm season of 2006 were smaller, with typical values around 30%. Rainfall rate variability for each of the three time periods shown in Figure 1 is tied to structure, motion and evolution of organized convective systems. The time scales associated with a storm element passing over a small urban catchment are similar to the time scales that are of most importance for runoff production and flood response in small urban catchments (Figure 1).

[6] Microstructure of rainfall rate is examined through analyses of the relationships between rainfall rate $R(t)$ and the raindrop shape process $\mu(t)$, scale $\Lambda^{-1}(t)$ and the scaled raindrop number density $N_0(t)$. The fundamental objective is to characterize stochastic properties of rainfall rate in terms of random processes representing time variation in numbers and sizes of raindrops, as represented through

$\{\mu(t), \Lambda(t), N_0(t)\}$. We also examine the dependence structure among the processes $\mu(t)$, $\Lambda^{-1}(t)$ and $N_0(t)$. The state estimation problem of reconstructing the unknown stochastic processes $\{\mu(t), \Lambda(t), N_0(t); t \in [0, T]\}$ from raindrop size distribution observations is a key element of the analysis methodology (section 2). Analyses of rainfall rate variability in section 3 utilize the "scaling law formulations" [*Sempere Torres et al.*, 1994; *Uijlenhoet and Stricker*, 1999; *Uijlenhoet et al.*, 2003a, 2003b] of raindrop size distributions as a framework (section 2).

[7] The central topic of this study is the microstructure of rainfall rate from organized convective systems that produce extreme rainfall rates. We also examine properties of the occurrence process of storms that produce extreme rainfall rates. Seasonal and diurnal cycles are key elements of the temporal occurrence process for heavy rainfall from organized convective systems. Convective intensity, as reflected in cloud-to-ground lightning observations, is an important feature of the diurnal and seasonal cycles of storm occurrences. Analyses are synthesized to highlight key issues in examining stochastic properties of rainfall rate.

2. Rainfall Rate: Marked Point Process Representations

[8] Analyses of rainfall rate as a stochastic process are based on a marked point process model [*Smith*, 1993; *Karr*, 1991] of raindrop size distributions. The marked point process represents the number and sizes of raindrops that pass a sample area of unit size (1 m^2), that is parallel to the ground surface during a convective storm element. The sample area reflects the scale of interest for relating rainfall rate to land surface processes, including infiltration and runoff production. In this section, we develop the stochastic model of raindrop size distributions in flux form, as described above, and translate it into a sample volume representation (1) using an assumed power law relationship for the terminal velocity of raindrops.

[9] Rainfall rate will be examined over a time interval $[0, T]$, which represents a time period containing one or more high rain rate convective elements. For the analyses of section 3, we will focus attention on a time period of 60 min. The time period is longer than the life cycle of an individual convective cell and corresponds to time scales over which temporal variability of rainfall rate controls flood response in "small" urban drainage basins [*Smith et al.*, 2005] (see also Figure 1).

[10] The arrival time (in s) of the ith drop during the time interval $[0, T]$ is denoted T_i and the diameter (in mm) of the ith drop (i.e., the diameter of a sphere of equivalent mass) is denoted D_i. The total number of drops during the time period $[0, T]$ is denoted M. With this notation $\{(T_i, D_i); i = 1, \ldots, M\}$ is a marked point process [see *Karr*, 1991] with $\{T_i, i = 1, \ldots, M\}$ a point process on the interval $[0, T]$, for which each point T_i is paired with the mark D_i.

[11] Rainfall accumulation (mm) at time t is given by

$$A(t) = \frac{\pi}{6}\ 10^{-6} \sum_{i=1}^{M(t)} {D_i}^3 \tag{3}$$

where $M(t)$ is the number of raindrops that have arrived by time t, $t \in [0, T]$:

$$M(t) = \sum_{i=1}^{M} 1(T_i\ \leq\ t) \tag{4}$$

The indicator function notation $1(T_i \leq t)$ denotes the random variable that takes the value 1 if $T_i \leq t$ and 0 otherwise.

[12] Rainfall rate (mm h^{-1}) is defined as

$$R(t) = 3600\ \left[\frac{A(t) - A(t - \Delta t)}{\Delta t}\right] \tag{5}$$

where Δt is the averaging time period. Because rainfall is intrinsically a point process, rainfall rate cannot be obtained as the limit of the term on the right-hand side of (5) as the time interval Δt decreases to 0. Rainfall rate can only be defined relative to a fixed averaging time interval Δt. The time interval used for analyses in the following section is 1 min. The median value of drop arrival rate from the Princeton observations (section 3) for rain rates greater than 1 mm h^{-1} is 1300 drops m^{-2} s^{-1}. The interquartile range of drop arrival rates extends from 800 to 2000 drops m^{-2} s^{-1} and the largest drop arrival rate during the 2006 observing period was 6950 drops m^{-2} s^{-1}.

[13] The counting process $M(t)$ specifies the number of raindrops that have arrived as a function of time. It is modeled as a Cox process [*Karr*, 1991; see also *Smith and Karr*, 1983; *Smith*, 1993], i.e., a Poisson process with randomly varying rate of occurrence $\{\lambda(u); u \geq 0\}$. In this case the conditional distribution of the counting process is

$$P\{M(t) = k \mid \lambda(u), u \leq t\} = \frac{\exp\left(-\int_0^t \lambda(u)\ du\ \right)\left(\int_0^t \lambda(u)\ du\right)^k}{k!} \tag{6}$$

where k is a nonnegative integer.

[14] The distribution of drop sizes is represented by a gamma distribution with randomly varying "shape" parameter $\eta(t)$ and "scale" parameter $\gamma(t)$ (for related analyses, see *Ulbrich*, 1983; *Tokay and Short*, 1996; *Bringi et al.*, 2003; *Narayana Rao et al.*, 2006; *Moisseev and Chandrasekar*, 2007, and references therein]. The probability density function of drop diameters takes the form

$$f(x \mid \eta(t), \gamma(t)) = \frac{1}{\Gamma(\eta(t))}\ x^{\eta(t)-1}\ \gamma(t)^{-\eta(t)} \exp\left(-\frac{x}{\gamma(t)}\right);\ x\ \geq\ 0 \tag{7}$$

where $\Gamma(s)$ is the gamma function. Of principal interest in this study are the stochastic processes $\{\lambda(t), \eta(t), \gamma(t)\}$, and their relationship to rainfall rate. Microstructure of rainfall rate is examined through analyses of distributional properties of the random processes representing drop arrival rate, "scale" of the raindrop size distribution and "shape" of the raindrop size distribution.

[15] Rainfall rate, based on the representations in (3)–(7), can be computed using the law of large numbers [*Smith*, 1993] in terms of the random processes representing drop

arrival rate, central tendency in drop diameter and shape of the DSD, yielding

$$R(t) = 6\pi\ 10^{-4}\ \lambda(t)\frac{\Gamma(\eta(t)+3)}{\Gamma(\eta(t))}\gamma(t)^3 \tag{8}$$

Analyses of rainfall rate center on the "state estimation" problem [see *Karr*, 1991] of estimating the time-varying stochastic processes $\{\lambda(t), \eta(t),\gamma(t)\}$ from observations of the marked point process $\{T_i, D_i\}$.

[16] The time-varying parameters of the gamma drop size distribution are estimated using both maximum likelihood (MLE) and moment of moments procedures. In both cases the estimator for the scale parameter $\gamma(t)$ takes the form

$$\hat{\gamma}(t) = \frac{\hat{m}(t)}{\hat{\eta}(t)} \tag{9}$$

where $\hat{m}(t)$ is the time-varying estimator of the mean diameter and $\hat{\eta}(t)$ is the estimator (either MLE or method of moments) of the shape parameter. For the method of moments procedure [*Mood et al.*, 1974] the estimator of the shape parameter is

$$\hat{\eta}(t) = \hat{c}(t)^{-2} \tag{10}$$

where $\hat{c}(t)$ is the sample estimator of the coefficient of variation (standard deviation divided by the mean) of the gamma distribution. Maximum likelihood estimators of the shape parameter follow procedures of *Venables and Ripley* [2002]. For the analyses in section 3, we use kernel estimators of the sample mean and standard deviation in which observations are binned into 1-min time intervals. Because of the large drop arrival rates and the 1-min averaging time, efficiency and bias issues do not play a major role in the state estimation problem. The state estimator for the conditional rate of occurrence process is

$$\hat{\lambda}(t) = \delta t^{-1}\sum_{i=1}^{M} 1(\| t - T_i \| \leq \delta t) \tag{11}$$

The estimator at time t is a local moment estimator of the mean arrival rate.

[17] It is conventional in radar meteorology and other areas of the atmospheric sciences to examine raindrop size distributions from a sample volume representation of the number and sizes of drops in a volume of the atmosphere, rather than from the flux representation presented above [see, e.g., *Waldvogel*, 1974; *Ulbrich*, 1983; *Doviak and Zrnic*, 1993]. The sample volume representation specifies the number of drops in a 3-D sample element which we take to be 1 m on a side. We denote the number of drops by M and the sizes $\{\tilde{D}_i\}$, $i = 1, \ldots, M$. Given a terminal velocity relationship in terms of drop sizes, it is straightforward to switch between flux and sample volume representations [*Smith*, 1993]. We use a power law terminal velocity relationship of the form

$$v(x) = v_0 x^p \tag{12}$$

with parameter values v_0 = 6 and p = 0.67 [*Atlas and Ulbrich*, 1977]. Vertical v within a thunderstorm cell can depart significantly from terminal velocity and these departures can play an important role in the distribution of surface rainfall rates [see, e.g., *Smith et al.*, 2005]. Departures from terminal velocity are generally smaller for near-surface conditions (see *Munchak and Tokay* [2008] for a recent discussion).

[18] Under the assumptions of the marked point process model, the number of drops has a Poisson distribution with parameter:

$$\tilde{\lambda}(t) = \frac{\lambda(t)}{v_o}\ \frac{\Gamma(\eta(t)-p)}{\Gamma(\eta(t))}\gamma(t)^{-p} \tag{13}$$

and the drop sizes have a gamma distribution of the form

$$g(x \mid \eta(t),\gamma(t)) = \frac{1}{\Gamma(\eta(t)-p)}\ x^{\eta(t)-p-1}\ \gamma(t)^{-(\eta(t)-p)} \cdot \exp\left(-\frac{x}{\gamma(t)}\right) \tag{14}$$

These results follow from the representations of *Smith* [1993].

[19] The distribution of drop counts and sizes is combined in the raindrop spectrum, $N(x)$, which represents the expected number of drops per cubic meter of sample volume per mm of drop diameter centered at a diameter of x mm [*Doviak and Zrnic*, 1993].

[20] The gamma drop spectrum can be represented as in (1) with

$$N_0(t) = \frac{\lambda(t)}{v_0 \cdot \gamma(t)^{\eta(t)}}\ \frac{1}{\Gamma(\eta(t))} \tag{15}$$

$$\Lambda(t) = \frac{1}{\gamma(t)} \tag{16}$$

$$\mu(t) = \eta(t) - p - 1 \tag{17}$$

The representation of rainfall rate in (2) follows from use of (15)–(17) in (8).

[21] "Scaling law" formulations of raindrop size distributions have provided important insights to rain rate fluctuations and useful tools for addressing remote sensing problems [*Sempere Torres et al.*, 1998; *Testud et al.*, 2001; *Uijlenhoet et al.*, 2003a, 2003b; *Uijlenhoet and Sempere Torres*, 2006]. The scaling law form of the raindrop size distribution is derived from representation of the raindrop spectrum in the form

$$N(x|\ R(t)) = R(t)^{\alpha} g\left(R(t)^{-\beta}x\right) \tag{18}$$

where $g(y)$ is the "general raindrop size distribution" (see the formulation of *Uijlenhoet et al.* [2003a, 2003b]).

[22] The gamma form of the scaling law follows from the assumption that

$$g(y) = \kappa\ y^{\mu}\exp(-cy) \tag{19}$$

Table 1. Summary of the 25 60-min Storm Periods[a]

Date	Time (UTC)	Max 1 Rain (mm h^{-1})	Max 15 Rain (mm h^{-1})	Max 60 Rain (mm h^{-1})	CV	μ	λ (m^{-2} s^{-1})	Diameter (mm)	CG Strikes
12 May	0242	42	17	10.9	0.87	8.8	4485	1.54	0
12 May	0345	57	21	7.8	1.78	6.1	3910	1.70	0
12 May	0421	45	9.2	5.3	1.70	6.2	3990	1.57	2
15 May	2318	27	15	4.6	1.52	5.3	3920	1.34	0
16 May	0043	83	26	6.5	2.48	7.4	3185	2.13	1
16 May	1048	37	18	12	0.62	7.4	3690	1.55	2
2 Jun	2332	41	14	4.3	1.78	4.2	1152	2.20	0
3 Jun	0021	115	51	15	1.94	6.0	4067	2.12	0
3 Jun	0348	81	49	18	1.18	8.7	5405	1.80	3
3 Jun	1644	126	29	7.8	2.75	6.1	4480	2.12	0
8 Jun	2318	60	35	10	1.60	7.8	3585	1.84	0
14 Jun	2327	64	36	13	1.39	7.6	3310	1.92	0
23 Jun	2314	63	32	9.4	1.61	6.8	3915	1.78	11
24 Jun	1034	59	20	4.9	2.82	7.8	4425	1.70	0
24 Jun	2254	40	14	5.4	1.40	10.3	3620	1.65	0
30 Jun	0246	36	17	7.1	1.43	8.8	3230	1.63	30
4 Jul	1957	48	22	5.8	2.01	6.9	2033	2.04	10
6 Jul	0712	59	15	5.5	1.84	5.17	2467	1.96	0
13 Jul	0234	107	38	11	2.10	11.6	6320	1.93	55
21 Jul	1939	26	9.2	2.7	2.12	13.0	2560	1.63	55
22 Jul	0006	88	61	18	1.47	9.8	4940	1.92	35
22 Jul	1954	92	27	8.1	2.36	13.1	5115	1.98	2
22 Jul	2047	120	78	29	1.25	12.1	6035	2.03	50
22 Jul	2247	39	12	4.2	1.94	6.8	4040	1.50	0
5 Oct	0401	123	66	26	1.29	7.8	4265	2.20	11

[a]Shown are date (day and month); time (UTC); maximum rain rate (mm h^{-1}) at 1-, 15- and 60-min time intervals; coefficient of variation of 1-min rainfall rate for the 60-min period; shape μ at maximum rainfall rate; drop arrival rate λ (drops m^{-2} s^{-1}) at maximum rain rate; mean diameter at maximum rain rate; and total CG strikes during the 60-min period.

It follows that

$$N(x|R(t)) = \kappa R(t)^{\alpha-\mu\beta} x^{\mu} \exp\left\{-cR(t)^{-\beta}x\right\} \tag{20}$$

[23] From the perspective of our model formulation, the key elements of the scaling law model are that the shape parameter does not vary over time and the scale parameter Λ and N_0 are power law functions of rainfall rate:

$$\mu(t) = \mu \tag{21}$$

$$N_0(t) = \kappa R(t)^{\alpha-\mu\beta} \tag{22}$$

$$\Lambda(t) = c\, R(t)^{-\beta} \tag{23}$$

with

$$\kappa = \left[6\pi\ 10^{-4}\ v_0\Gamma(4+p+\mu)\right]^{-1} c^{4+p+\mu} \tag{24}$$

It follows that $N_0(t)$ is a power law function of $\Lambda(t)$. The assumption of a constant shape parameter is a strong one, which we examine through analyses of the Princeton data below. More generally, it is important to examine the role of temporal variability of the shape parameter in controlling stochastic properties of rainfall rate.

[24] The gamma scaling law model provides a parsimonious representation of rainfall rate. The shape parameter is constant and the scale eter can be expressed as a deterministic function of r vice versa). This representation of the raindrop size distribution is especially important for radar rainfall estimation, providing a solid foundation for estimating rainfall rate from a single variable, the radar reflectivity factor. *Brandes et al.* [2004] explored similar issues in the framework of radar rainfall estimation on the basis of assumed gamma raindrop size distributions. They argue that the dimensionality of the gamma parameterization can be reduced from 3 to 2 through functional relationships between the shape $\mu(t)$ and scale $\Lambda(t)$. These distributional issues highlight fundamental aspects of rainfall rate variability that are examined in the next section through application of the gamma model to raindrop size distributions from heavy convective rainfall events.

3. Results

[25] Analyses in this section utilize raindrop size distribution measurements from a Joss-Waldvogel disdrometer [*Joss and Waldvogel*, 1967; see also *Steiner and Smith*, 2000] that was deployed in Princeton, New Jersey during the period May–October 2006. Analyses focus on 25 time periods (60 min duration) for which peak 1-min rainfall rates exceeded 25 mm h^{-1} (Table 1). Each of the 25 time periods in Table 1 represents a separate storm episode for which peak rain rates exceed 25 mm h^{-1}, but drop to 0 between events. There were periods in the May–October time window when the disdrometer was not operating, most notably a three week period in August.

[26] The definition of heavy rain used in this study is motivated by an underlying representation of the occurrence of heavy rain periods. In this formulation, rainfall rate can be represented by $\{U_i, R_i(t); t \in [0, L_i], i = 1, \ldots, M_j\}$, where M_j is the number of rainfall periods during year j, U_i is the time

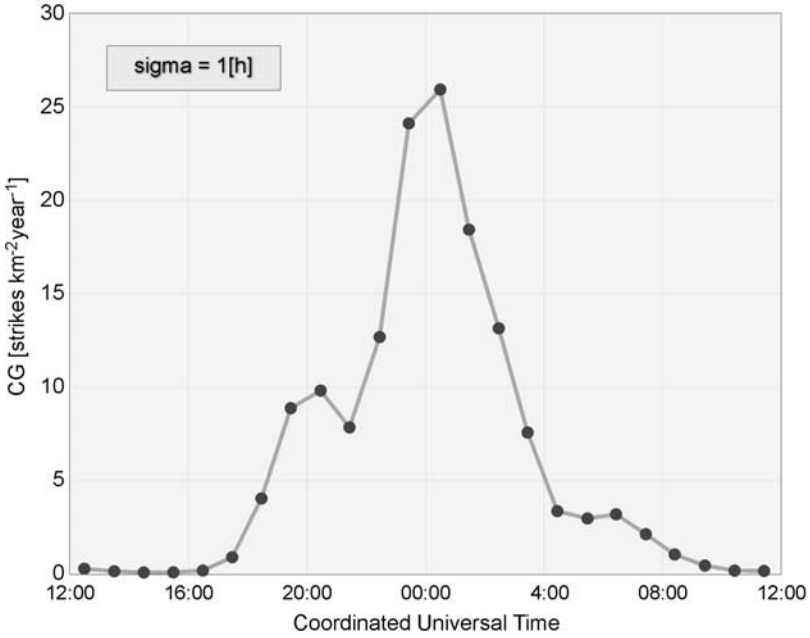

Figure 2. Diurnal cycle of CG lightning (CG strikes km^{-1} a^{-1}) for May–October for Princeton, New Jersey (10 km radius around the Princeton disdrometer station), based on NLDN observations from 1991 to 2006. Frequency estimators are constructed using a Gaussian smoothing procedure with smoothing parameter (''sigma'') of 60 min.

occurrence (the initial time of positive rainfall rates) of the *i*th storm period during the year, $R_i(t)$ is the rainfall rate at time t relative to the occurrence time U_i and L_i is the duration of the *i*th rainfall period. We focus on heavy convective rainfall by ''thinning'' the underlying process of rainfall occurrence to include only rain periods with maximum rainfall rates exceeding a high threshold. For the analyses presented below we use a 1-min threshold of 25 mm h^{-1}. The focus of analyses presented below is on variability of raindrop size distributions within a rain period and their control on the microstructure of rainfall rate. We also examine the links between the occurrence process of rain periods and microstructure of rainfall rate, especially through nonstationarities tied to the diurnal and seasonal cycles of convective rainfall.

[27] The diurnal cycle of convection plays a central role in the distribution of extreme short-term rainfall rates. The diurnal cycle in the occurrence of extreme rainfall rates is closely linked to the diurnal cycle of thunderstorms in Princeton (Figure 2; represented as a flash density in CG strikes km^{-2} a^{-1}). The CG flash density is near 0 for a time period extending from 1000 to 1600 UTC. The CG flash density is greater than 10 strikes km^{-2} a^{-1} for a 5-h window centered around 0000 UTC. For reference, the mean annual lightning flash density for Princeton is 3.0 strikes km^{-2} a^{-1}. The occurrence of heavy rain periods from the sample of 25 events closely reflects the diurnal cycle of lightning with no events during the period 1200–1600 UTC and 21 of 25 events occurring between 1900 UTC and 0600 UTC. For the subsequent analyses, we define a ''day'' to extend from 1200 to 1200 UTC to reflect the diurnal cycle of convection and its control on rainfall rate distribution.

[28] The seasonal cycle of convection also plays an important role in the distribution of extreme rainfall rates. Mean CG flash densities h sharp peak in July at a rate that is an order of magnitude larger than the winter minimum (figure not shown). The most intense convection for the 25 storm periods, as reflected in CG flash density, was concentrated during the midsummer period (Table 1).

[29] There were three heavy rain periods from 1200 UTC on 22 July through 1200 UTC on 23 July, including the period with peak 15 min (78 mm h^{-1}) and 60 min (29 mm h^{-1}) rainfall rates during the observing period (Table 1). The 60-min storm period on 22 July with peak rainfall rate at 2047 UTC (Figures 1, 3, and 4) produced the largest flood peak in Harry's Brook (Figure 1), which drains the urban core of Princeton, New Jersey (see Figure 4), during a three year stream gauging period. During the 6-min period from 2041 to 2047 UTC on 22 July, the estimated shape parameter μ increased from 7.8 to 12.1 as rainfall rate increased from 38 mm h^{-1} to the maximum rainfall rate of 120 mm h^{-1}. During the same time period, the estimated scale parameter Λ^{-1} decreases uniformly and N_0 increases.

[30] This period of peak rainfall rates on 22 July 2006 was produced by a rapidly moving multicell thunderstorm (Figure 4), which was embedded in a larger mesoscale convective system. The evolution of individual convective cells within a storm element plays an important role in the microstructure of rainfall rate (see *Smith et al.* [2005] for additional discussion; future studies will examine microstructure of rainfall rate through combined analyses of disdrometer and radar observations). The two rain periods which precede and follow the 60-min period with maximum rain rate (Table 1) were elements of the same mesoscale convective system. The temporal correlation structure in the occurrence of storm periods at a location is linked to the spatial organization of mesoscale convective systems, as illustrated in Figure 4. The 25 events during the 2006 observing period were clustered into 15 days (defining a ''day'' to extend

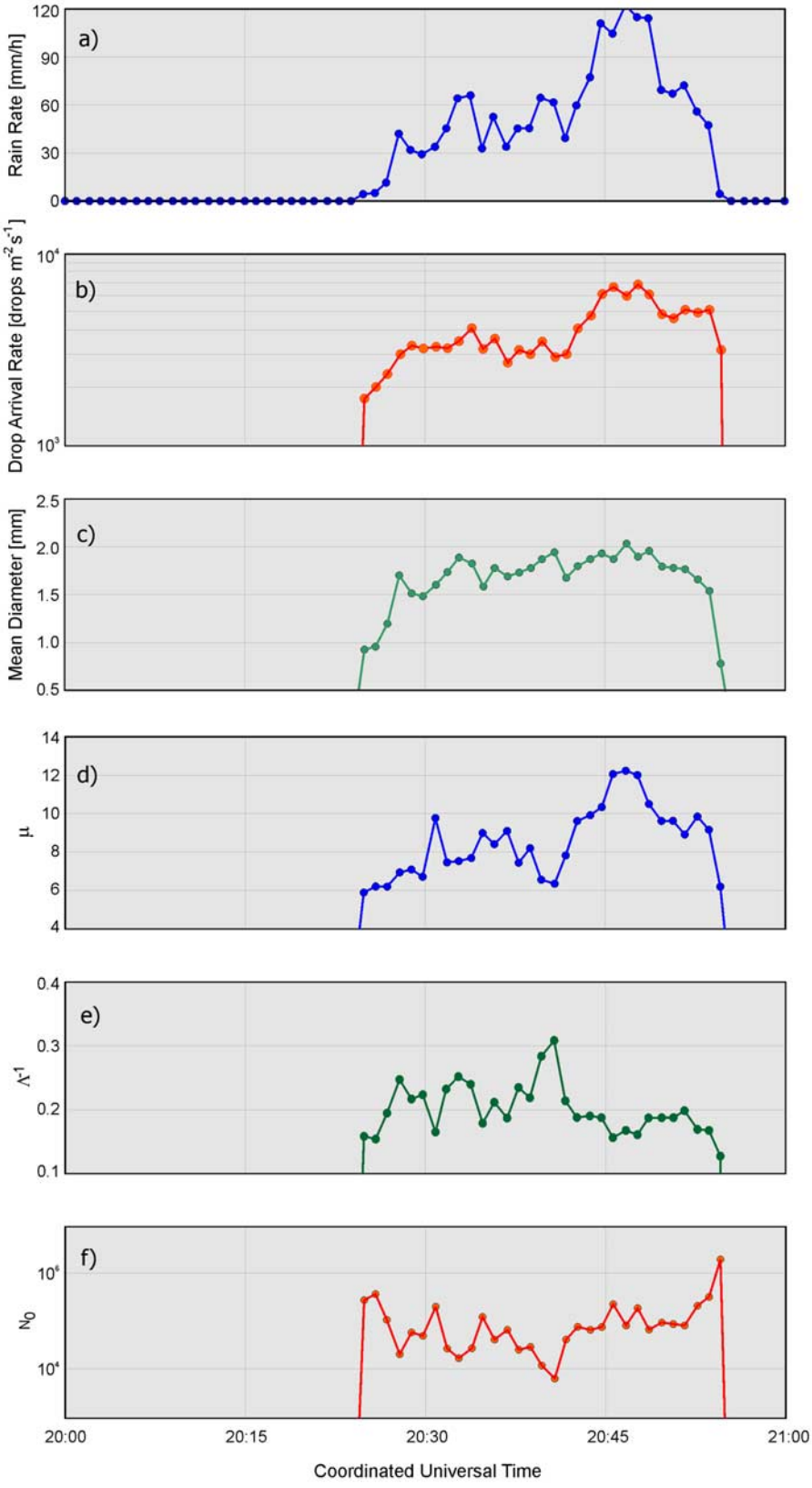

Figure 3. Time series of (a) rainfall rate (mm h^{-1}), (b) drop arrival rate (drops m^{-2} s^{-1}), and (c) mean diameter (mm) and state estimates of (d) μ, (e) Λ^{-1} (mm), and (f) N_0 (drops m^{-3} $mm^{-(1+\mu)}$) for the 60-min period (see Table 1) on 22 July 2006 with peak 60-min rainfall accumulation.

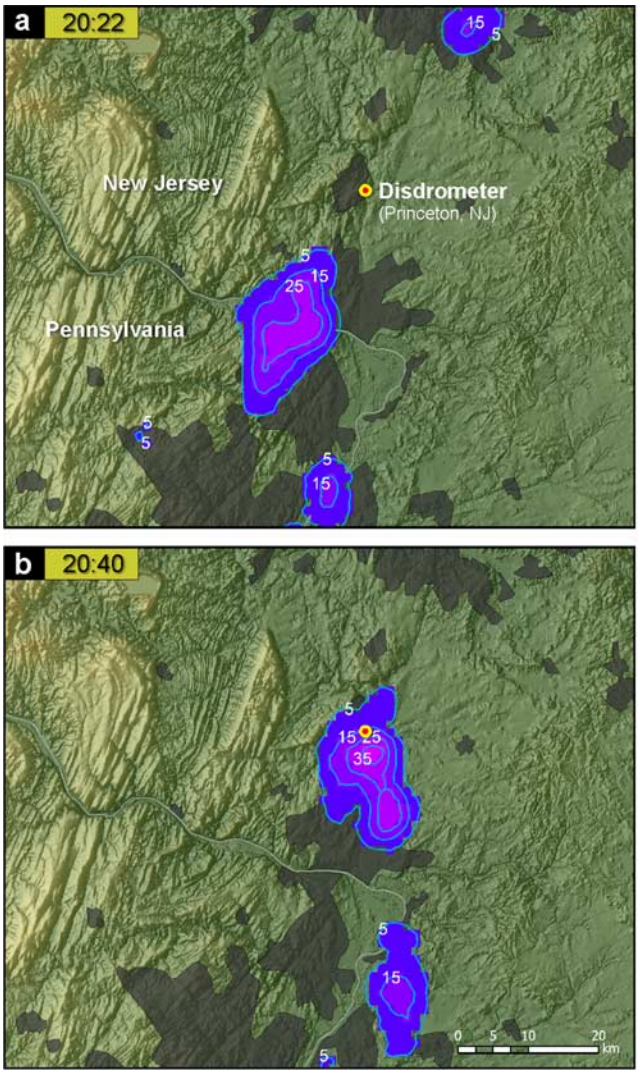

Figure 4. HydroNEXRAD rainfall rate fields for 22 July 2006 at (top) 2022 and (bottom) 2040 UTC on 22 July 2006. Location of the Princeton disdrometer is shown. "Urban" land use is highlighted in brown, and shading highlights topography of the surrounding region in New Jersey and Pennsylvania.

from 1200 UTC to 1200 UTC, as noted above) during which one or more 60-min storm periods occur over the day. Paired studies of point rainfall rate using disdrometers and radar provide useful tools for examining microstructure of point rainfall rate and linking microstructure of rainfall rate to structure and evolution of mesoscale convective systems.

[31] The summary analyses in Table 1 are for 60-min time periods containing the peak 1-min rain rates and with the beginning time chosen to give the maximum 60-min rainfall rate. Rain rate distributions are summarized by maximum 1-min, 15-min and 60-min rainfall rates, coefficient of variation of 1-min rainfall rates for the 60-min time window (i.e., standard deviation of 1-min rainfall rates divided by mean 1-min rainfall rates), the shape parameter μ corresponding to the maximum 1-min rainfall rate, the drop arrival rate λ corresponding to the maximum 1-min rainfall rate, the mean diameter cor ding to the maximum 1-min rainfall rate and the numb loud-to-ground (CG) lightning strikes within 10 km of the disdrometer during the 60-min period.

[32] Using equation (2) with the reconstructed stochastic processes ($\lambda(t)$, $\eta(t)$, $\gamma(t)$) results in near-perfect reconstruction of rainfall rate (Figure 5) for the 2006 Princeton data. Thus the information contained in the drop size measurements for a given minute can be condensed to the three gamma parameters, maintaining an almost perfect representation of rainfall rate. Inferences are not tied to estimation procedure. Method of moments and maximum likelihood procedures for estimating size distribution parameters provide similar estimates (Figure 6).

[33] The relationships between the state variables $\mu(t)$, $\Lambda(t)$ and $N_0(t)$ and rainfall rate R(t) are summarized through box plots (Figure 7) representing the conditional distribution of drop spectrum parameters given the rainfall rate. Rainfall rate is divided into 7 categories, less than 5 mm h^{-1}, 5–10 mm h^{-1}, 10–20 mm h^{-1}, 20–40 mm h^{-1}, 40–60 mm h^{-1}, 60–80 mm h^{-1} and greater than 80 mm h^{-1}.

[34] Dependence of the estimated state variables $\mu(t)$, $\Lambda(t)$ and $N_0(t)$ on rainfall rate is strongest for the shape parameter μ (Figure 7). Median values of μ increase systematically with rainfall rate and variability in μ decreases with increasing rain rate, most notably for rain rates greater than 40 mm h^{-1}. For rainfall rates less than 5 mm h^{-1} (Figure 7), the shape parameter μ has a median value just less than 4, an interquartile range from 2.2 to 6.1 and extremes ranging from just less than 0 to just above 12. For rain rates greater than 80 mm h^{-1}, the median value of μ increases to 8, and the interquartile range (6.3 to 9.6) and extremes (4.2 to 11.5) are narrower.

[35] Estimators of the scale parameter Λ^{-1} and N_0 vary with rain rate, but in more subtle fashion (Figure 7). There is a tendency for the central portion of the scale parameter distribution to increase with rain rate and a more pronounced decrease in variability of the scale parameter with rain rate. Similarly, the central portion of state estimators of N_0

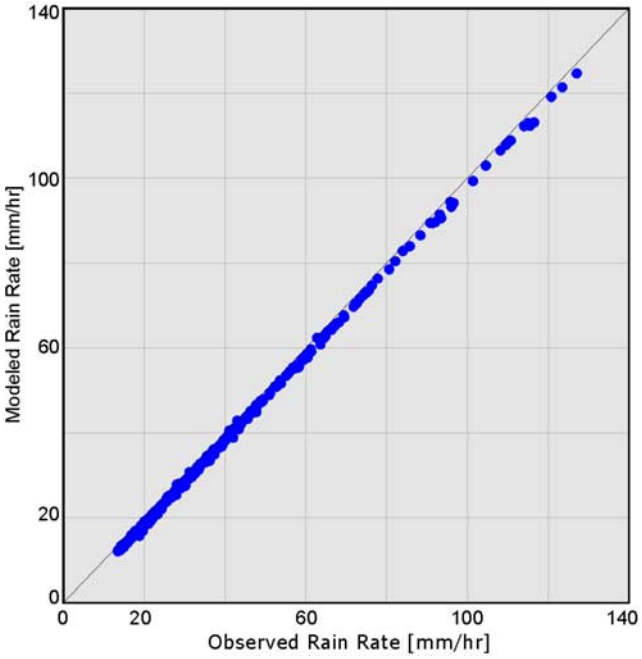

Figure 5. Model rain rate computed from equation (2) versus observed rain rate for the 2006 Princeton data.

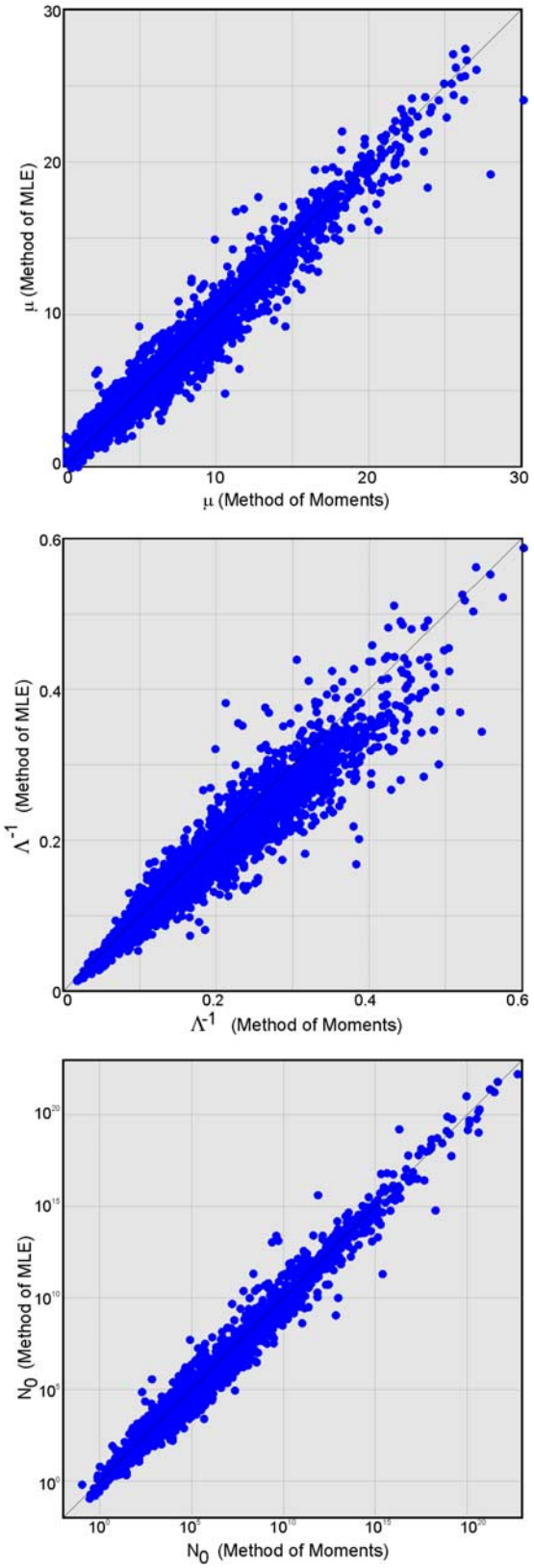

Figure 6. Scatterplots of maximum likelihood versus method of moments state estimates of (top) μ, (middle) Λ^{-1}, and (bottom) N_0.

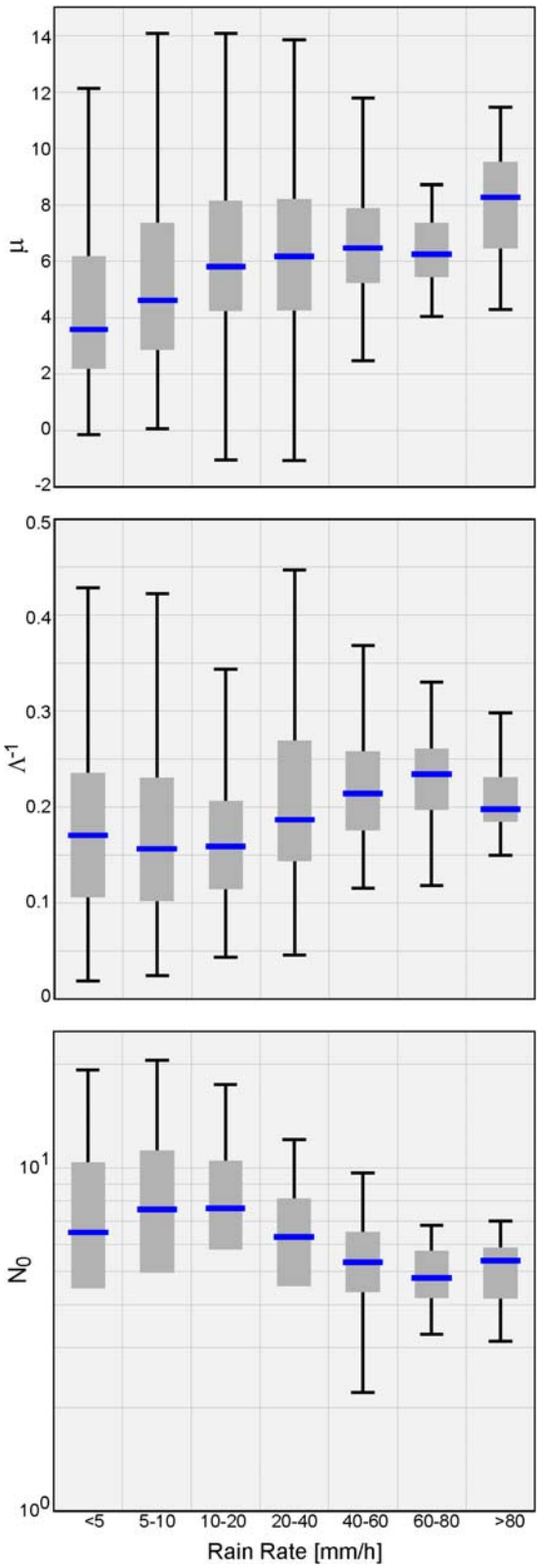

Figure 7. Box plots of state estimates of (top) μ, (middle) Λ^{-1}, and (bottom) N_0. The distributions of state estimators for each of the parameters are represented by box plots of estimates for rain rate (1) less than 5 mm h^{-1}, (2) between 5 and 10 mm h^{-1}, (3) between 10 and 20 mm h^{-1}, (4) between 20 and 40 mm h^{-1}, (5) between 40 and 60 mm h^{-1}, (6) between 60 and 80 mm h^{-1}, and (7) greater than 80 mm h^{-1}.

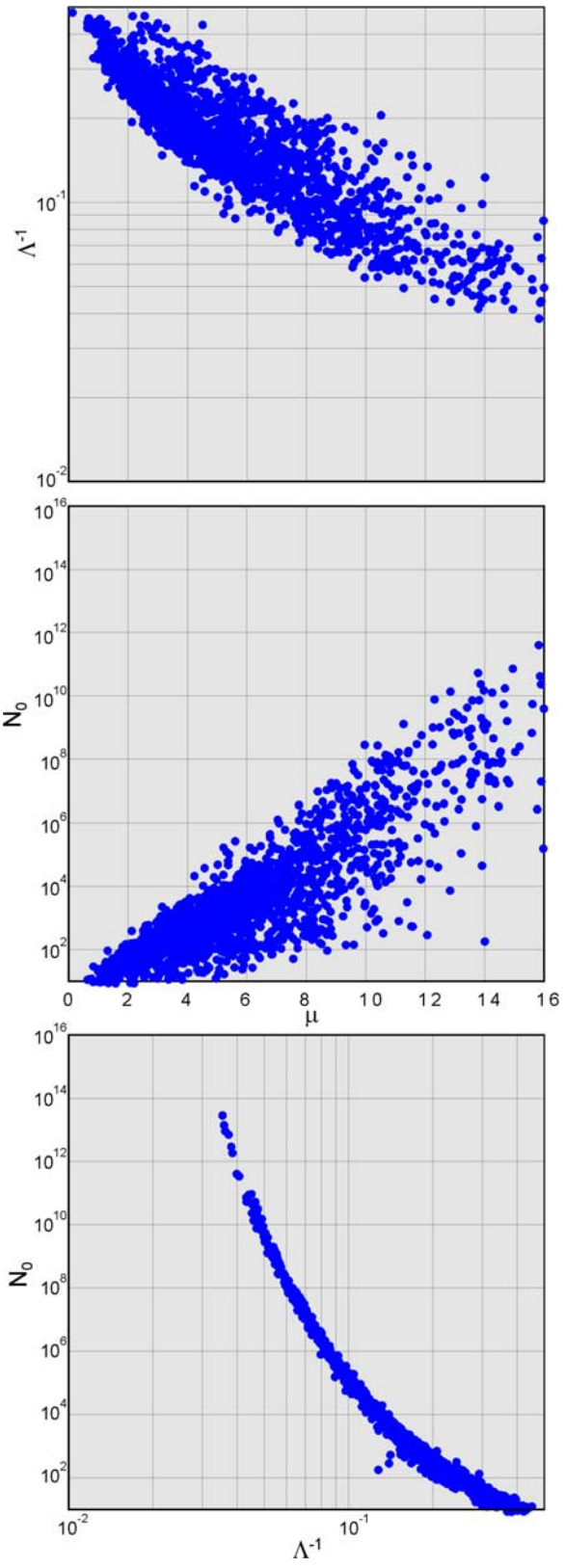

Figure 8. Dependence among the state estimators of gamma model parameters, represented through scatterplots of state estimators of (top) Λ^{-1} versus μ, (middle) N_0 versus μ, and (bottom) N_0 versus Λ^{-1}.

generally decrease with rain rate and the variability of the estimators decreases.

[36] There is strong dependence among the state estimators of $\mu(t)$, $\Lambda(t)$ and $N_0(t)$ (Figure 8). The scale parameter Λ^{-1} decreases systematically with increasing scale μ and N_0 increases linearly with μ. There is also strong dependence between N_0 and Λ^{-1}, with estimators of N_0 decreasing with increasing Λ^{-1}. These analyses suggest that the "dimensionality" of variability in raindrop size distributions is less than 3 for heavy convective rain. Preceding analyses (Figure 5) show that information on numbers and sizes of raindrops can be condensed to the 3 three parameters of the gamma drop spectrum. The dependence among the three processes shown in Figure 8 indicates that a more parsimonious representation can be achieved. Radar rainfall algorithms that use a single variable, radar reflectivity factor, to estimate rainfall rate work best when the dimensionality can be collapsed to 1, as in the case of the scaling law model [*Krajeswki and Smith*, 2002]. Analyses of the Princeton data suggest that for heavy convective rainfall, the dimensionality of variation in raindrop size distributions is greater than 1 and that variation in the shape parameter μ is significant.

[37] Time evolution of the shape of the raindrop size distribution is an important feature of rainfall rate variability of heavy convective rainstorms in Princeton and this variation is tied to the intensity of convection. For heavy convective rainfall, the estimated shape parameter varies over the course of an event (Figure 3) and there is systematic variation from event to event (Table 1). The largest values of the peak scale parameter (Table 1) are concentrated during the July events on days with intense convection, as represented by the number of CG lightning strikes. Smaller values of the peak scale parameter (Table 1) are concentrated on days with weaker convection. Extreme values of the shape parameter are not simply tied to extreme rainfall rates, but also reflect convective intensity. Peak 1-min rainfall rates exceeding 100 mm h^{-1} exhibit a range of peak scale parameters that are linked to CG lightning flash density (Table 1); note in particular contrasts between the 2–3 June, 3–4 June, 22–23 July and 4–5 October events.

[38] Intermittency of rainfall rate is a central feature of any characterization of rainfall variability. The largest values of coefficient of variation for the 60-min storm periods are associated with short bursts of large rainfall rates. The 22 July event peaking at 1954 UTC has a peak 1-min rainfall rate of 92 mm h^{-1} and a 60-min rainfall rate of 8.1 mm h^{-1}. The CV of 1-min rainfall rates for the 60-min period is 2.36 (fourth largest in the sample of 25 events). An important element of the microstructure of rainfall rate that is closely tied to intermittency and variability of rainfall rate is duration of extreme rainfall rates. For the three flood events highlighted in Figure 1 duration of rainfall rates greater than 25 mm h^{-1} ranged from 8 min for the 2 June event to 27 min for 22 July event. Intermittency of rainfall rate, as well as other distributional properties of raindrop size distributions, are closely linked to the structure, motion and evolution of convective elements in organized thunderstorm systems (Figure 4).

4. Summary and Conclusions

[39] A stochastic model of raindrop size distributions is used to analyze the temporal variability of rainfall rate for

heavy convective rainfall. Analyses are used to examine the microstructure of rainfall rate at time scales that are important for land surface processes associated with infiltration and runoff production. The stochastic model of rainfall rate is based on a model of raindrop size distributions in which the drop spectrum has a gamma distribution with model parameters that are time-varying stochastic processes. State estimation procedures are developed for estimating the time-varying parameters of the gamma drop spectrum from measured raindrop size distributions. The model is used to analyze rain rate variability from disdrometer observations in Princeton, New Jersey during the period May–October 2006. Analyses focus on a sample of 60-min periods with heavy rainfall. The principal conclusions of the study are the following.

[40] 1. The model of rainfall rate based on the time-varying gamma drop spectrum model (equation (2)), in combination with state estimation procedures, provides accurate reconstruction of rainfall rate. This implies that the information about rainfall rate that is contained in a complete representation of the number and sizes of raindrops can be condensed to three values, the shape, μ, scale, Λ^{-1} and normalized number density N_0 parameters of the Gamma drop spectrum. Sensitivity of these inferences to the details of the state estimation procedure was examined by comparison of results for both maximum likelihood and method of moments state estimation procedures. Both state estimation procedures provide excellent representation of rainfall rate and similar estimates of the time-varying model parameters. Future studies should examine estimation properties for additional parametric models of raindrop size distributions and parameter estimation procedures [see, e.g., *Haddad et al.*, 1996; *Smith and Kliche*, 2005], as well as sensitivity to instrument properties [see, e.g., *Tokay et al.*, 2005].

[41] 2. An important feature of the estimation results for the Princeton data is the dependence of the scale parameter μ on rainfall rate. For the 25 storm periods during the 2006 observing period, the estimate of μ at the peak rainfall rate varies from 4.2 to 13.1. The scale parameter Λ^{-1} and N_0 exhibit a more complex dependence on rainfall rate. There is not, however, a strong power law relationship between Λ^{-1} and rainfall rate or between N_0 and rainfall rate. Analyses provide insights to the links between microstructure of rainfall rate and stochastic variation in properties of the raindrop size distribution. Future studies should examine additional methods for characterizing temporal variation in raindrop size distributions [see, e.g., *Testud et al.*, 2001] and explore their links to rainfall microstructure.

[42] 3. There is strong dependence among the time-varying model parameters, $\mu(t)$, Λ^{-1} (t) and $N_0(t)$. The scale parameter $\Lambda^{-1}(t)$ decreases with increasing shape $\mu(t)$ and the normalized number density $N_0(t)$ increases with $\mu(t)$. There is also strong dependence between scale and normalized number density, with $N_0(t)$ decreasing for increasing $\Lambda^{-1}(t)$.

[43] 4. The diurnal and seasonal cycles of convection plays a prominent role in determining the upper tail of the distribution of rainfall rate. The 25 storm events of 60 min duration during the 2006 observing period in Princeton are clustered in a time window that extends from afternoon until early morning. This mimics the diurnal cycle of CG lightning for Princeton. Analyses suggest that convective intensity, as reflected in CG lightning ensities, may be an important element in determining raindrop size distributions. Variation of the shape parameter (item 3 above) is linked to convective intensity, with larger values of the peak shape parameter associated with CG flash densities.

[44] 5. The temporal variability of 1-min rainfall rate during heavy convective rain periods is large, as reflected in a variety of measures. Only 2 of the 25 storm periods have a coefficient of variation of rainfall rate for the 60-min period that is less than 1. Short-term variability of rainfall rate plays an important role in infiltration and runoff processes linked to flood hydrology in many settings, especially in small urban watersheds. For 60-min time periods, short-term variability of convective rainfall is fundamentally linked to the structure and motion of convective storm elements. Future studies will examine the role of storm evolution from a Lagrangian perspective (i.e., following a convective element) in determining distributional properties of rainfall rate and associated processes tied to the raindrop size distribution.

[45] 6. Microstructure of extreme rainfall rates is closely tied to the structure of organized convective systems and the distribution of rainfall rate at a point for a storm period is tied to structure and evolution of the convective element. The occurrence process of storm periods with extreme rainfall rates exhibits diurnal and seasonal cycles and exhibits correlation that is linked to the structure and evolution of organized convective systems. Analyses that combine high-resolution radar measurements of the time evolution of the 3-D structure of organized convective systems with high time resolution measurements of raindrop size distributions provide important directions for further examination of the microstructure of extreme rainfall rates.

[46] **Acknowledgments.** NLDN data provided by the NASA Lightning Imaging Sensor (LIS) instrument team and the LIS data center via the Global Hydrology Resource Center (GHRC) located at the Global Hydrology and Climate Center (GHCC), Huntsville, Alabama, through a license agreement with Global Atmospherics, Inc. (GAI). The data available from the GHRC are restricted to LIS science team collaborators and to NASA EOS and TRMM investigators. The research was supported by the National Science Foundation (grants EEC 0540832, EAR-0409501, BES-0607036, EF-0709538, and ITR-0427325) and NASA.

References

Atlas, D., and C. W. Ulbrich (1977), Path- and area-integrated rainfall measurement by microwave attenuation in the 13 cm band, *J. Appl. Meteorol.*, *16*, 1322–1331.

Brandes, E. A., G. Zhang, and J. Vivekanandan (2004), Drop size distribution retrieval with polarimetric radar: Model and applications, *J. Appl. Meteorol.*, *43*, 461–475.

Bringi, V. N., V. Chandrasekar, J. Hubbert, E. Gorgucci, W. L. Randeu, and M. Schoenhuber (2003), Raindrop size distribution in different climatic regimes from disdrometer and dual-polarized radar analysis, *J. Atmos. Sci.*, *60*(2), 354–365.

Celia, M. A., E. T. Bouloutas, and R. L. Zarba (1990), A general mass-conservative numerical solution for the unsaturated flow equation, *Water Resour. Res.*, *26*(7), 1483–1496.

Doviak, J. D., and D. S. Zrnic (1993), *Doppler Radar and Weather Observations*, 2nd ed., Academic, San Diego, Calif.

Haddad, Z. S., S. L. Durden, and E. Im (1996), Parameterizing the raindrop size distribution, *J. Appl. Meteorol.*, *35*, 214–228.

Joss, J., and A. Waldvogel (1967), Ein Spektrograph fuer Niederschlagstropfen mit automatischer Auswertung, *Pure Appl. Geophys.*, *68*, 240–246.

Karr, A. F. (1991), *Point Processes and their Statistical Inference*, 2nd ed., Marcel Dekker, New York.

Krajeswki, W. F., and J. A. Smith (2002), Radar hydrology: Rainfall estimation, *Adv. Water Resour.*, *25*, 1387–1394.

Moisseev, D. N., and V. Chandrasekar (2007), Examination of the $\mu\,\delta$ relation suggested for drop size distribution parameters, *J. Atmos. Oceanic Technol.*, *24*, 847–855, doi:10.1175/JTECH2010.1.

Mood, A. M., F. A. Graybill, and D. C. Boes (1974), *Introduction to the Theory of Statistics*, 3rd ed., 577 pp., McGraw-Hill, New York.

Munchak, S. J., and A. Tokay (2008), Retrieval of raindrop size distributions from simulated dual-frequency radar measurements, *J. Atmos. Oceanic Technol.*, *47*, 223–239, doi:10.1175/2007JAMC1524.1.

Narayana Rao, T., N. V. P. Kirankumar, B. Radhakrishna, and D. Narayana Rao (2006), On the variability of the shape-slope parameter relations of the gamma raindrop size distribution model, *Geophys. Res. Lett.*, *33*, L22809, doi:10.1029/2006GL028440.

Orville, R. E., and G. R. Huffines (2001), Cloud-to-ground lightning in the United States: NLDN results in the first decade, 1989–98, *Mon. Weather Rev.*, *129*(5), 1179–1193.

Sempere-Torres, D., J. M. Porr, and J. D. Creutin (1994), A general formulation for rain drop size distribution, *J. Appl. Meteorol.*, *33*, 1494–1502.

Sempere-Torres, D., J. M. Porr, and J.-D. Creutin (1998), Experimental evidence of a general description for raindrop size distribution properties, *J. Geophys. Res.*, *103*, 1785–1797.

Smith, J. A. (1993), A marked point process model of raindrop size distributions, *J. Appl. Meteorol.*, *32*, 284–296.

Smith, J. A., and A. F. Karr (1983), A point process model of summer season rainfall occurrences, *Water Resour. Res.*, *19*(1), 95–103.

Smith, J. A., A. J. Miller, M. L. Baeck, P. A. Nelson, G. T. Fisher, and K. L. Meierdiercks (2005), Extraordinary flood response of a small urban watershed to short duration convective rainfall, *J. Hydrometeorol.*, *6*(5), 599–617.

Smith, P. L., and D. V. Kliche (2005), The bias in moment estimators for parameters of drop size distribution functions: Sampling from the exponential distributions, *J. Appl. Meteorol.*, *44*, 1195–1205, doi:10.1175/JAM2258.

Steiner, M., and J. A. Smith (2000), Reflectivity, rain rate, and kinetic energy flux relationships based on raindrop spectra, *J. Appl. Meteorol.*, *39*, 1923–1940.

Steiner, M., and J. A. Smith (2004), Scale-dependence of radar rainfall rates—An assessment based on raindrop spectra, *J. Hydrometeorol.*, *5*(6), 1171–1180.

Steiner, M., J. A. Smith, and R. Uijlenhoet (2004), A microphysical interpretation of radar reflectivity–rain rate relationships, *J. Atmos. Sci.*, *61*(10), 1114–1131.

Testud, J., S. Oury, R. A. Black, P. Amayenc, and X. Dou (2001), The concept of "normalized" distribution to describe raindrop spectra: A tool for cloud physics and cloud remote sensing, *J. Appl. Meteorol.*, *40*, 1118–1140.

Tokay, A., and D. A. Short (1996), Evidence from tropical raindrop spectra of the origin of rain from stratiform versus convective clouds, *J. Appl. Meteorol.*, *35*, 355–371.

Tokay, A., P. G. Bashor, and K. R. Wolff (2005), Error characteristics of rainfall measurements by collocated Joss-Waldvogel disdrometers, *J. Atmos. Oceanic Technol.*, *22*, 513–527.

Ulbrich, C. W. (1983), Natural variations in the analytical form of the raindrop size distribution, *J. Clim. Appl. Meteorol.*, *22*, 1764–1775.

Uijlenhoet, R., and D. Sempere-Torres (2006), Measurement and parameterization of rainfall microstructure, *J. Hydrol.*, *328*, 1–7.

Uijlenhoet, R., and J. N. M. Stricker (1999), A consistent rainfall parameterization based on the exponential raindrop size distribution, *J. Hydrol.*, *218*, 101–127.

Uijlenhoet, R., M. Steiner, and J. A. Smith (2003a), Variability of raindrop size distributions in a squall line and implications for radar rainfall estimation, *J. Hydrometeorol.*, *4*(1), 43–61.

Uijlenhoet, R., J. A. Smith, and M. Steiner (2003b), The microphysical structure of extreme precipitation, *J. Atmos. Sci.*, *60*, 1220–1238.

Venables, W. N., and B. D. Ripley (2002), *Modern Applied Statistics with S*, 4th ed., Springer, New York.

Waldvogel, A. (1974), The No jump of raindrop spectra, *J. Atmos. Sci.*, *31*, 1067–1078.

Williams, G. A., and C. T. Miller (1999), An evaluation of temporally adaptive transformation approaches for solving Richards equation, *Adv. Water Resour.*, *22*, 831–840.

Zipser, E. J., D. J. Cecil, C. Liu, S. W. Nesbitt, and D. P. Yorty (2006), Where are the most intense thunderstorms on Earth?, *Bull. Am. Meteorol. Soc.*, *87*, 1057–1071.

M. L. Baeck, E. Hui, A. A. Ntelekos, and J. A. Smith, Department of Civil and Environmental Engineering, Princeton University, Princeton, NJ 06544, USA. (jsmith@princeton.edu)

W. F. Krajewski, IIHR-Hydroscience and Engineering, University of Iowa, Iowa City, IA 52242, USA.

M. Steiner, Research Applications Laboratory, National Center for Atmospheric Research, P.O. Box 3000, Boulder, CO 80307-3000, USA.